

Generation of Cell-Instructive Collagen Gels through Thermodynamic Control

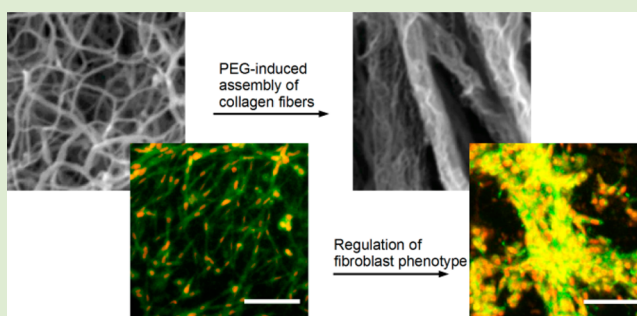
Youyun Liang,^{†,‡} Hyunjoon Kong,[‡] and Yen Wah Tong^{*,†}

[†]Department of Chemical and Biomolecular Engineering, National University of Singapore, Singapore 117576, Singapore

[‡]Department of Chemical and Biomolecular Engineering, University of Illinois, Urbana–Champaign, Urbana, Illinois 61801, United States

Supporting Information

ABSTRACT: Recent studies have demonstrated the usefulness of three-dimensional hydrogel scaffolds for cell instruction. However, the control of gel architectures in cell-friendly conditions remains a challenge. Here, we report a novel method to generate unique three-dimensional collagen gel structures for the modulation of cell phenotypes. This was achieved by directing collagen self-assembly with unreactive hydrophilic polyethylene glycol (PEG) chains. Our approach allowed the fiber sizes and mechanics of three-dimensional collagen gels to be readily controlled. It also enabled the recapitulation of distinctive structures such as large perimysial collagen cables. Through different experiments, we elucidated the underlying mechanism for this PEG-mediated thermodynamic regulation of gel structure. We further used these cell-instructive three-dimensional gels to bring about pronounced morphological changes in encapsulated fibroblasts and their activation to form contractile bundles. Overall, our platform fills a gap in the existing array of collagen scaffolds and can potentially be adapted to a variety of self-assembling systems.



Collagen gels have been widely used for cell culture and to direct cell behavior.^{1–4} To generate these cell-instructive matrices, the mechanical properties of collagen gels were typically modified by various methods such as chemical cross-linking and change of collagen concentrations.^{1–4} However, these methods may be associated with several drawbacks, such as the limited variety of gel architectures and decreasing permeability with increased gel stiffness.⁵ Emerging studies have also shown that, although bulk mechanical properties are important in regulating cell phenotypes, it is the microstructures that better relate to the length scales of cell sensing.^{6,7} As such, the successful application of three-dimensional (3D) cell-instructive gels greatly depends on the ability to generate unique gel structures under mild, cell-friendly processing conditions. Here, we report a method to control the microstructure of 3D cell-encapsulating collagen gels via incorporation of polyethylene glycol (PEG) into the collagen pregel solutions before subsequent activation of gel formation. With this cell-friendly approach, we were able to directly tune the self-assembly of collagen molecules during cell encapsulation. This method also allowed the generation of unique gel architectures resembling perimysial collagen cables in muscles. We further demonstrated that the unique gel architectures produced with this method resulted in the activation of encapsulated fibroblasts into proto-myofibroblasts. These phenotypic changes could not be observed with

unmodified collagen gels and collagen gels formed by other approaches such as covalent cross-linking.

First, we regulated the self-assembly of collagen gels by using different mass ratios of hydrophilic PEG to collagen ($M_{\text{PEG-COL}}$) during gel formation. Increasing $M_{\text{PEG-COL}}$ from 0 to 25 led to a corresponding increase in mean diameters (d) of fibers from 90 to 300 nm, as shown in the SEM images (Figure 1a,b). At $M_{\text{PEG-COL}}$ of 25, we were able to generate gels consisting of fibers with similar diameters to perimysial collagen cables that surround muscle fibers (Figures 1a and S1).⁸ As a comparison, we also fabricated covalently cross-linked collagen gels by using a bifunctional cross-linker, PEG-di(succinic acid *N*-hydroxy-succinimidyl ester) (PEG-diNHS; Figure S1). The structures resembling perimysial cables were reproducible by these chemically cross-linked control gels (Figure S1).

As the total collagen concentration was fixed for all $M_{\text{PEG-COL}}$, the increase of the collagen fiber diameter resulted in increasing mesh size (ξ), from 1.1 to 3.0 μm as seen from the SEM images (Figure 1b). In contrast, the chemically cross-linked control hydrogel formed from mixture of collagen and PEG-diNHS exhibited reduced porosity as compared to the pure collagen gel (Figure S1).

Received: October 3, 2013

Accepted: November 18, 2013

Published: November 26, 2013

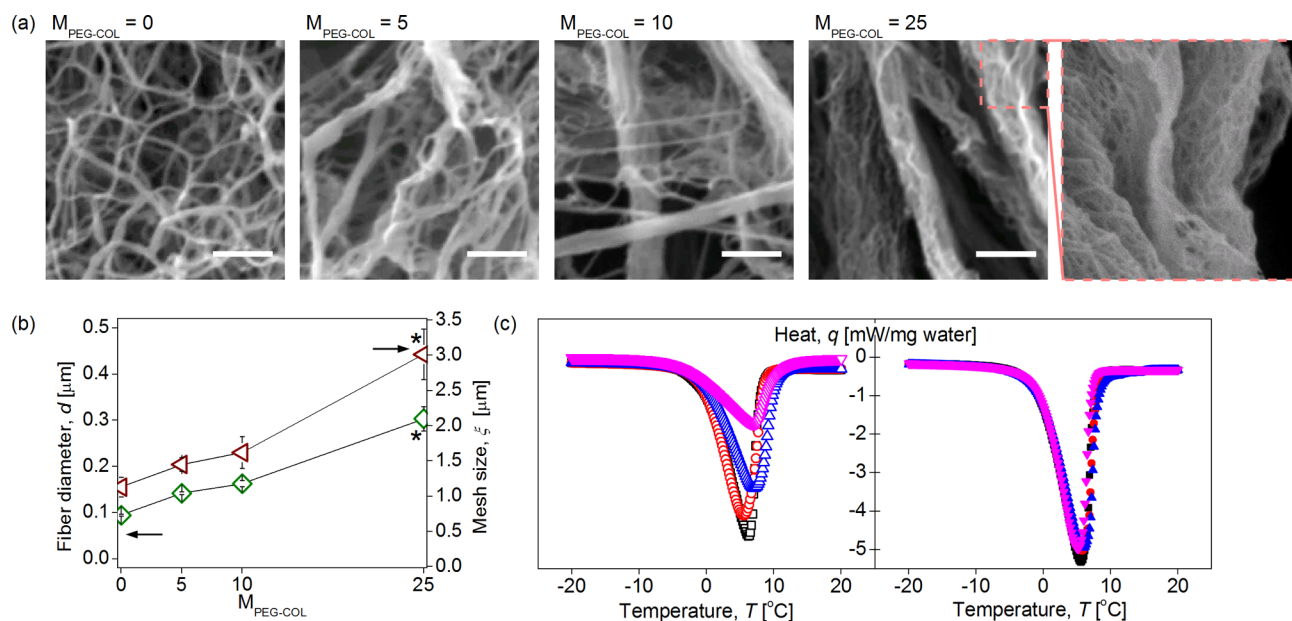


Figure 1. Structure of cell-instructive collagen gels formed by thermodynamic control. (a) Increasing the mass ratio of PEG to collagen ($M_{\text{PEG-COL}}$) increased fiber diameters. The collagen gels formed by thermodynamic control had distinct architecture from chemically cross-linked control gels (Figure S1). Also, the size of the collagen fiber bundles in $M_{\text{PEG-COL}} = 25$ resembled that of perimysial collagen cables found in muscles (Figure S1; scale bars represent $1 \mu\text{m}$, inset magnified $4\times$). (b) The increase in $M_{\text{PEG-COL}}$ from 0 to 25 resulted in an increase in the mean fiber diameter (d ; green diamond) and mesh size (ξ ; open red triangle). (c) Increasing $M_{\text{PEG-COL}}$ from 0 (open black square) to 5 (open red circle), 10 (open blue triangle), and 25 (open pink triangle) reduced water's melting endothermic peaks in pregel solutions. This indicated increased proportions of unfreezable bound water. However, following complete self-association of the collagen fibrils to form fibers, the melting endotherms were uniform for all $M_{\text{PEG-COL}}$ from 0 (solid black square) to 5 (solid red circle), 10 (solid blue diamond), and 25 (solid pink diamond), thus, indicating no disparity in bound water fraction (bars represent standard error; *single-factor ANOVA test, $\alpha < 0.01$).

To investigate the mechanism by which PEG regulates the collagen fiber diameters, we further characterized the intermolecular interactions with Fourier transform infrared spectroscopy (FTIR) and differential scanning calorimeter (DSC). First, FTIR was used to investigate if hydrogen bonding was present between collagen and PEG gel mixtures. As there was no shift in the amide bands of collagen gels with the incorporation of PEG, we can conclude that there was limited hydrogen bonding between collagen and PEG (Table S1).^{9,10} Second, DSC was used to determine the relative ratios of free water and hydrogen-bonded, bound water for different $M_{\text{PEG-COL}}$ before and after gelation. A higher fraction of unfreezable bound water would lead to a smaller endothermic peak during melting.¹¹ According to the DSC analysis, an increase in $M_{\text{PEG-COL}}$ from 0 to 25 resulted in a reduction in the endothermic peak in the pregel solutions (Figure 1c). However, following gelation, there were no major differences in the areas of the endothermic peaks between different $M_{\text{PEG-COL}}$ (Figure 1c).

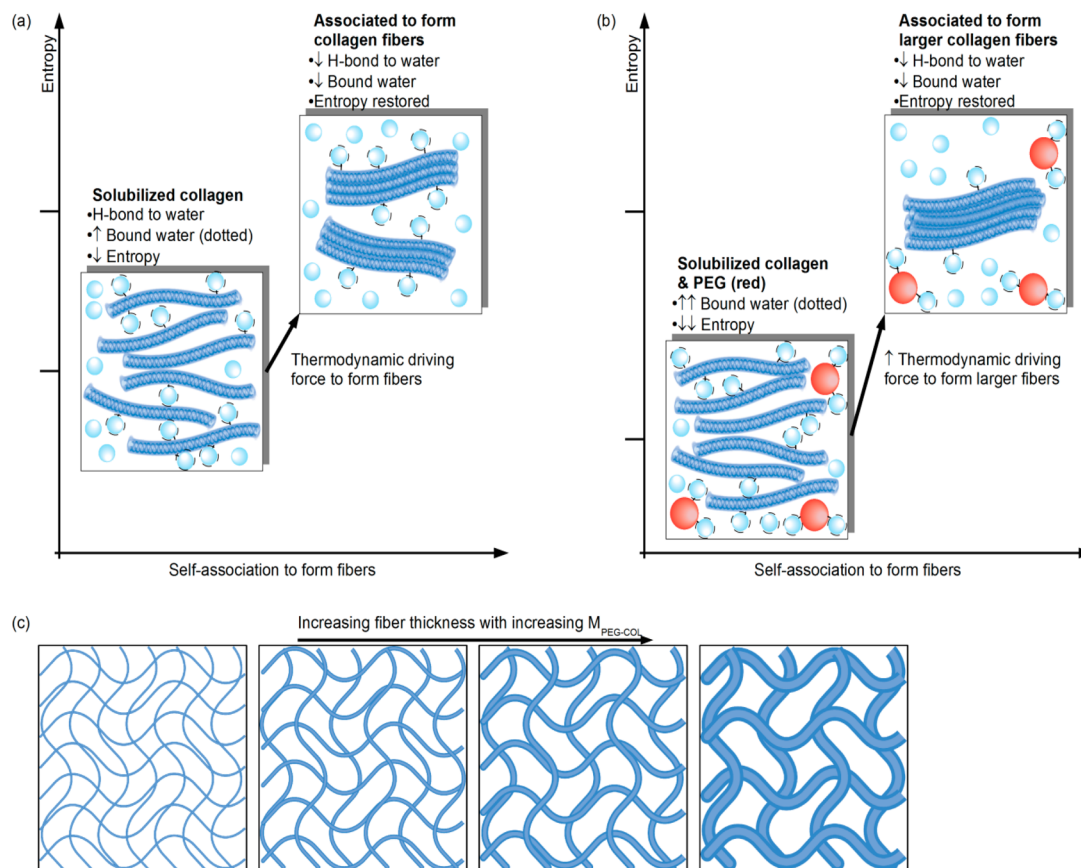
The calorimetric analysis demonstrated that solubilized collagen molecules in the pregel solution formed extensive hydrogen bonds with water, which decreased the overall entropy due to the lowered motility of the bound water. This reduced entropy drove the collagen molecules to self-assemble into fibers bundles. It had been previously reported that, during such self-assembly, new hydrogen bonds formed between collagen molecules at the expense of collagen–water hydrogen bonds.¹² Due to the larger number of water molecules, the gain in entropy due to the release of bound water far outweighed the loss of entropy due to collagen association, thus favorable entropy was restored (Scheme 1a). Furthermore, the DSC analysis disclosed that the addition of the long, hydrophilic

PEG chains further increased the amount of bound water in the pregel solutions. This result indicated that PEG addition further lowered initial entropy of the pregel solution, thus generating a larger driving force for the formation of larger collagen fiber bundles (Scheme 1b).

We further investigated the effect of PEG on the mechanical properties of the bulk gels and the comprising fibers. The bulk rigidity was quantified by measuring the storage moduli (G') of the gels subjected to low-amplitude oscillatory shear deformation. As $M_{\text{PEG-COL}}$ was increased from 0 to 5 and 10, a corresponding decrease in G' was observed (Figure 2a). However, further increase of $M_{\text{PEG-COL}}$ from 10 to 25 resulted in the increase of G' from approximately 2 to 6 Pa. This complex change in G' with varying $M_{\text{PEG-COL}}$ could be attributed to the simultaneous changes in fiber diameter and spacing.¹³ It had been shown that an increase in spacing between fibers resulted in the reduction of G' , but a significant increase in fiber diameter contributed to increasing G' .¹⁴ The G' of pure PEG solution was almost zero, indicating that the incorporated PEG chains did not make a direct contribution to the gel mechanics (Figure 2a).

The bending rigidity (κ) of the individual collagen fiber was quantified from G' and ξ using the MacKintosh model (details presented in Experimental Section).¹⁴ According to the model, κ is directly proportional to the square root of ($G'\xi^5$). Unlike the bulk storage modulus which had complex changes with different $M_{\text{PEG-COL}}$, the κ values increased with $M_{\text{PEG-COL}}$ due to the increasing fiber diameters (Figure 2b).

Although there were different trends for the bulk gel storage modulus and single fiber mechanical properties, we expected that cells cultured within the gels were more greatly affected by single fiber stiffness due to their similar length scales.^{15,16} It had

Scheme 1. Regulation of Collagen Structure through Addition of PEG^a

^a(a) Under gel-forming conditions, the large proportion of H-bonded bound water (dotted), decreased the overall entropy of the system, providing the thermodynamic driving force for self-association of fibrils. Fiber bundle formation subsequently reduced the bound water fraction and restored overall entropy of the system. (b) With the incorporation of hydrophilic PEG (red spheres), the proportion of bound water further increased, thus, creating lower entropy and an even larger larger driving force for fibril self-association. As such, the size of the resultant collagen fibers increased. (c) Fiber thickness and mesh size were expected to increase with the mass ratio of hydrophilic PEG chains to collagen ($M_{\text{PEG-COL}}$).

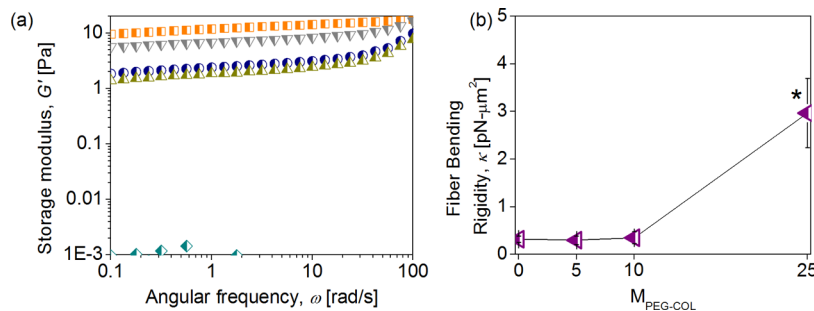


Figure 2. Mechanics of cell-instructive collagen gels formed by thermodynamic control. (a) As $M_{\text{PEG-COL}}$ was increased from 0 (square/orange) to 5 (circle/black), and 10 (up-facing triangle/brown), the storage modulus (G') decreased. However, further increase of $M_{\text{PEG-COL}}$ to 25 (down-facing triangle/gray) resulted in an increase in G' . This complex trend could be attributed to the concurrent changes in mesh size and fiber rigidities. G' of pure PEG solution (tilted square/green) was close to zero, indicating negligible contribution to chain entanglement. (b) The fiber bending rigidities (κ ; left-facing triangle/purple) increased with $M_{\text{PEG-COL}}$ due to increasing fiber diameters (bars represent standard error; *single-factor ANOVA test, $\alpha < 0.01$).

been shown in previous studies that cells were only able to sense the mechanical properties within the order of micrometers.^{15,16} Apart from the generation of unique gel architecture, another notable feature of this mode of control was the increase in mesh size from 1.1 to 3.0 μm with increasing fiber rigidity. The rigidity of hydrogels was conventionally increased by increasing either polymer concentration or cross-linking densities.^{1–4} This typically led to a

decrease in mesh size and could be associated with compromised mass transfer and reduced viability of encapsulated cells.^{5,17} However, this reduction in mesh size was not a concern in our system.

Fibroblasts were incorporated into the collagen gel presenting the unique perimysial cables-like architecture ($M_{\text{PEG-COL}} = 25$) in order to examine the effects of modified fiber structures on cellular phenotype and organization. The

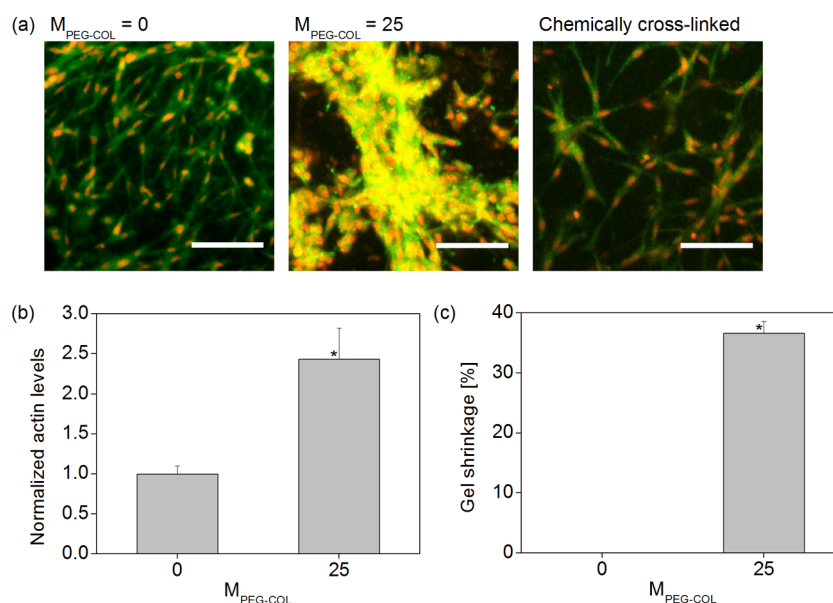


Figure 3. Regulation of fibroblast phenotype through cell-instructive collagen gels formed by thermodynamic control. (a) Fibroblasts cultured within the respective gels for 10 days were stained to reveal the nuclei (red) and actin filaments (green). Fibroblasts in pure collagen gels ($M_{\text{PEG-COL}} = 0$) were spindle-shaped and formed interconnected networks while those in PEG-containing gels ($M_{\text{PEG-COL}} = 25$) aggregated to form fibroblast bundles resembling proto-myofibroblasts. This phenotype was not observed in the chemically cross-linked control gels (scale bars represent $50 \mu\text{m}$). (b) The fibroblasts in the PEG-containing gel had a higher level of normalized actin expression. (c) The fibroblasts in PEG-containing gels contracted the gels extensively, while no contraction was observed in pure collagen gels (bars represent standard error; *Student's t-test, $\alpha < 0.05$ in (b) and $\alpha < 0.01$ in (c)).

cells were loaded into the different hydrogels by mixing them with pregel solutions and subsequently incubating the mixtures at physiological temperature and pH to activate gel formation. The hydrophilic PEG chains were then removed by washing. Throughout culture for 10 days, the fibroblasts in pure collagen gels retained their spindle-shaped morphology and exhibited limited cell–cell adhesion. Such cellular organization was commonly observed when fibroblasts were cultured in soft, cell-adhesive hydrogels, such as Matrigel.¹⁸ Interestingly, fibroblasts encapsulated in collagen-PEG gel prepared at $M_{\text{PEG-COL}}$ of 25 formed large cell bundles with extensive cell–cell contact (Figure 3a,b). These fibroblast bundles bear resemblance to contractile proto-myofibroblast, which are commonly found during wound healing.^{19,20} Additionally, the normalized actin levels of fibroblasts in the PEG-containing gels was approximately 2.5 times of myofibroblasts (Figure 3b).^{19,20} After completion of the cell culture over 10 days, the contractile functions of the fibroblasts in gels prepared at varied $M_{\text{PEG-COL}}$ were further examined by measuring the degree of gel shrinkage. The collagen-PEG gel prepared at $M_{\text{PEG-COL}}$ of 25 underwent 38% more shrinkage than the pure collagen gel. This result indicated that the fibroblast bundles generated higher contractile function than their counterparts with limited cell–cell contact (Figure 3c).

To confirm that PEG molecules in the hydrogel during gel formation did not directly influence the cellular organization, we further encapsulated fibroblasts in pure collagen gels and incubated the cell–gel constructs in media supplemented with PEG. The addition of PEG after stable gel formation did not result in differences in cellular morphology (Figure S2). Separately, cells cultured in media supplemented with PEG exhibited minimal differences of cellular metabolic activity as characterized with reduction of 3-(4,5-dimethylthiazol-2-yl)-2,5-diphenyltetrazolium bromide (MTT; Figure S3). We therefore interpret that the morphological changes should be

attributed to the local fiber stiffness tuned with the PEG chains. Previous studies reported the activation of quiescent fibroblasts when cultured on substrates with increased rigidity.²¹ However, unlike the two-dimensional studies, our 3D configuration allowed extensive reorganization and formation of bundles with good cell–cell contacts.

In summary, through the incorporation of nonreactive PEG molecules, we were able to generate unique gel structures not reproducible by chemical cross-linking. We were also able to achieve increased stiffness of individual collagen fibers, accompanied with increasing mesh size. Through the control of hydrogel structure mediated by thermodynamic forces, we were able to regulate the cues for fibroblasts activation. As this study only examines the feasibility of PEG-mediated thermodynamic control for generation of cell-instructive collagen gels, further characterizations in terms of gene and protein expression have to be carried out to determine the underlying mechanisms. Overall, this study was the first to demonstrate that thermodynamic control could be used to generate unique cell-instructive scaffolds during cell encapsulation. This mode of control could potentially be applied to other self-assembling gels such as peptide and fibrin.

EXPERIMENTAL SECTION

Extended experimental procedures can be found in the Supporting Information. Materials were ordered from Sigma-Aldrich, unless otherwise specified.

Pure collagen gels and chemically cross-linked collagen gels were synthesized by using a previously established method.¹ For the synthesis of PEG-modified collagen gels through thermodynamic control, PEG-diOH (M_w 7500) was dissolved in DI water at a concentration of 300 mg/mL. The solution was then added to the collagen/DMEM/reconstituting solution mixture at different $M_{\text{PEG-COL}}$ before incubation at 37°C for 1 h. The synthesized gels were imaged by SEM (JSM-5600VL, JEOL) for analysis of mean fiber diameters and mesh sizes. FTIR (Shimadzu FTIR-8400) and DSC (Mettler

Toledo DSC) characterizations were also carried out to investigate the mechanism of collagen gel structure regulation. The gels' storage moduli (G') were further quantified by a rheometer (ARG2, TA Instruments). Following which, the average bending rigidities (κ) of the fibers were calculated by using the MacKintosh model from the following equation:¹⁴

$$\kappa = \sqrt{G' \xi^5 k T} \quad (1)$$

, where G' is the storage modulus in Pa, ξ is the mesh size in μm , k is the Boltzmann constant, and T is the temperature in K.

For the cell culture experiments, suspended mouse fibroblast cell lines L929 (ATCC) was mixed with appropriate solutions to form pure collagen hydrogels or PEG-containing modified hydrogels with final cell density of 500 cells/ μL . After incubation, the samples were rinsed thrice and fresh media was added. Media was exchanged once every 3 days. Following 10 days of culture, the gels were fixed and stained according to standard procedures and imaged with the confocal microscope (Nikon C1) for visualization of nuclei and actin filaments. The images obtained were further analyzed by ImageJ for quantification of actin expression. The final areas of the different gels were also tabulated and normalized by the initial gel areas to give the percentage gel shrinkage.

■ ASSOCIATED CONTENT

● Supporting Information

Supplementary figures and experimental procedures. This material is available free of charge via the Internet at <http://pubs.acs.org>.

■ AUTHOR INFORMATION

Corresponding Author

*Phone: (65) 6516-8467. Fax: (65) 6779-1936. E-mail: chetyw@nus.edu.sg.

Notes

The authors declare no competing financial interest.

■ ACKNOWLEDGMENTS

This work was supported by the National University of Singapore under Grant Nos. R279000328112 and R279000353112. The authors would like to thank Anjaneyulu Kodali for his help in the cell culture experiments.

■ REFERENCES

- (1) Liang, Y.; Jeong, J.; DeVolder, R. J.; Cha, C.; Wang, F.; Tong, Y. W.; Kong, H. *Biomaterials* **2011**, *32*, 9308–9315.
- (2) Paszek, M. J.; Zahir, N.; Johnson, K. R.; Lakins, J. N.; Rozenberg, G. I.; Gefen, A.; Reinhart-King, C. A.; Margulies, S. S.; Dembo, M.; Boettiger, D.; Hammer, D. A.; Weaver, V. M. *Cancer Cell* **2005**, *8*, 241–254.
- (3) Tierney, C. M.; Haugh, M. G.; Liedl, J.; Mulcahy, F.; Hayes, B.; O'Brien, F. J. *J. Mech. Behav. Biomed. Mater.* **2009**, *2*, 202–209.
- (4) Watanabe, K.; Nakamura, M.; Okano, H.; Toyama, Y. *Restor. Neurol. Neurosci.* **2007**, *25*, 109–117.
- (5) Kraehenbuehl, T. P.; Langer, R.; Ferreira, L. S. *Nat. Methods* **2011**, *8*, 731–736.
- (6) Discher, D. E.; Janmey, P.; Wang, Y. *Science* **2005**, *310*, 1139–1143.
- (7) Jacot, J. G.; Dianis, S.; Schnell, J.; Wong, J. Y. *J. Biomed. Mater. Res., Part A* **2006**, *79*, 485–494.
- (8) Gillies, A. R.; Lieber, R. L. *Muscle Nerve* **2011**, *44*, 318–331.
- (9) Sionkowska, A.; Skopinska-Wisniewska, J.; Wisniewski, M. *J. Mol. Liq.* **2009**, *145*, 135–138.
- (10) Sionkowska, A. *Polym. Degrad. Stab.* **2006**, *91*, 305–312.
- (11) Lee, K. Y.; Ha, W. S. *Polymer* **1999**, *40*, 4131–4134.
- (12) Parkinson, J.; Kadler, K. E.; Brass, A. J. *Mol. Biol.* **1995**, *247*, 823–831.

(13) Dagdas, Y. S.; Tombuloglu, A.; Tekinay, A. B.; Dana, A.; Guler, M. O. *Soft Matter* **2011**, *7*, 3524–3532.

(14) Branco, M. C.; Nettesheim, F.; Pochan, D. J.; Schneider, J. P.; Wagner, N. J. *Biomacromolecules* **2009**, *10*, 1374–1380.

(15) Buxboim, A.; Rajagopal, K.; Brown, A. E. X.; Discher, D. E. *J. Phys.: Condens. Matter* **2010**, *22*, 194116.

(16) Maloney, J. M.; Walton, E. B.; Bruce, C. M.; Van Vliet, K. J. *Phys. Rev. E: Stat., Nonlinear, Soft Matter Phys.* **2008**, *78*, 041923.

(17) Weber, L. M.; Lopez, C. G.; Anseth, K. S. *J. Biomed. Mater. Res., Part A* **2009**, *90*, 720–729.

(18) Serban, M. A.; Liu, Y.; Prestwich, G. D. *Acta Biomater.* **2008**, *4*, 67–75.

(19) Hinz, B. *J. Invest. Dermatol.* **2007**, *127*, 526–537.

(20) Hinz, B.; Pittet, P.; Smith-Clerc, J.; Chaponnier, C.; Meister, J. J. *Mol. Biol. Cell* **2004**, *15*, 4310–4320.

(21) Balestrini, J. L.; Chaudhry, S.; Sarrazy, V.; Koehler, A.; Hinz, B. *Integr. Biol.* **2012**, *4*, 410–421.